

# Tuning of Microwave Absorption Properties and Electromagnetic Interference (EMI) Shielding Effectiveness of Nanosize Conducting Black-Silicone Rubber Composites over 8–18 GHz

Raj K. Jani<sup>1, 2</sup>, Manoj K. Patra<sup>1</sup>, Lokesh Saini<sup>1</sup>, Anuj Shukla<sup>1</sup>,  
Chandra P. Singh<sup>1</sup>, and Sampat R. Vadera<sup>1, \*</sup>

**Abstract**—In this paper, studies on broadband microwave absorption and electromagnetic shielding effectiveness are reported in flexible rubber composites with low filler content of nanosize conducting carbon over 8–18 GHz frequency range of electromagnetic spectrum. Rubber based composites are prepared by loading of 1–15 wt% nanosize conducting Carbon Black (CB) in silicone rubber matrix. Effect of percentage loading of nanosize CB on DC conductivity, dielectric & microwave absorption properties and electromagnetic Shielding Effectiveness (SE) of silicone rubber composites is studied. The percolation threshold is achieved at low concentration (3 wt%) of CB in composites. The observed complex permittivity values revealed that composites with concentration of 5 wt% CB can provide more than 90% microwave absorption (Reflection Loss > -10 dB) over 8–18 GHz at composite thickness of 1.9–2.7 mm. Further, composites with concentration of 15 wt% of CB shows -40 dB SE over the broad frequency range 8–18 GHz at thickness 2.8 mm. The effect of composite thickness on microwave absorption properties and shielding effectiveness is also analyzed. Thus, the prepared rubber composites with suitable concentration of nanosize CB as filler may be used as microwave absorber in stealth applications as well as for EMI shielding of electronic equipments in various civilian and military areas.

## 1. INTRODUCTION

Flexible microwave absorbing composites are essentially required in military and civilian applications for reduction of radar signatures of airborne platforms/targets to achieve stealthy features as well as for protection of manpower & equipments from EM hazards. Rubber based composites with significant microwave absorption and shielding effectiveness have attracted the attention of the scientific community due to their advantages such as flexibility to cover curved structures, cut and paste type in nature, and weather resistant for outdoor applications. Ideally, promising composites should be thin, light weight and environmentally stable having wide absorption bandwidth coverage. In last few decades, various magnetic and carbonaceous materials have been used as fillers in composites to obtain microwave absorption and EMI shielding properties [1–3]. However, magnetic fillers based composites suffer from weight penalty due to their high density. Further, different carbon allotropes viz. carbon nanotubes (CNTs), carbon fibers (CFs) and graphene based composites also have certain difficulties including dispersion of filler in host matrix, reproducibility of functional properties, production of bulk quantity and cost effectiveness, thereby, limiting their extensive practical applications [4–11].

Nanosize conducting black (CB) is one of the promising filler materials due to its excellent electrical conductivity, light weight and low cost. There are several reports on the use of CB along with certain

---

*Received 27 February 2017, Accepted 18 May 2017, Scheduled 24 July 2017*

\* Corresponding author: Sampat Raj Vadera (svadera59@gmail.com).

<sup>1</sup> Defence Laboratory, Defence R&D Organization, Jodhpur-342011, Rajasthan, India. <sup>2</sup> Department of Physics, Jai Narain Vyas University, Jodhpur-342011, Rajasthan, India.

other filler materials in composites to achieve MW absorption properties [12–14]. In previous studies, this material has also been used by different researchers to obtain high Shielding Effectiveness (SE) in composites [15–17]. However, as per available literature it is seen that the use of CB alone as a microwave absorbing filler is not much explored. The authors could achieve SE values of  $\sim -30$  dB with high loading of carbon black  $\sim 50$  parts per hundred (phr) in gigahertz frequency range. Although an SE of  $\sim -40$  dB has been reported in some of composites by using elongated fillers viz. Ni fibers, Steel fibers, Ni filaments, etc. [18–20], inclusion of these types of fillers in the matrix brings difficulty in fabrication processes leading to inconsistency in properties.

Dispersion of filler is one of the biggest challenges, particularly at high concentration. This may lead to variation of functional properties, weakening the mechanical properties, increasing the cost and weight penalty of composites. Therefore, development of lightweight, flexible composites is highly crucial for many of the civil and defence applications, particularly for airborne systems.

In this work, attempts are made to develop flexible composites by taking nanosize CB as the only filler material in a room temperature curable silicone rubber matrix having broadband microwave absorption properties and EMI shielding effectiveness at low filler concentration. The percolation threshold of composites is achieved at very low concentration (3 wt%) of nanosize CB in these composites. Microwave absorption properties and shielding effectiveness of composites with different concentrations of CB are investigated at microwave frequencies over 8–18 GHz.

## 2. MATERIALS AND METHODS

### 2.1. Preparation of Composites

Ketjenblack conducting carbon black (CB) (produced by AkzoNobel Functional Chemicals, USA) with surface area  $800 \text{ m}^2/\text{g}$  (BET) and pore volume (dibutylphthalate)  $310\text{--}345 \text{ ml}/100 \text{ g}$  has been used as a filler for achieving desired electromagnetic performance in the rubber composites. Silicone rubber (purchased from Performance Polymers, Bangalore, India) has been used as a binder matrix for preparation of composites. This matrix has viscosity  $\sim 20 \text{ PaS}$ , density  $\sim 1.07 \text{ g/cc}$ , dielectric constant  $\sim 3$ , dielectric loss tangent  $\sim 0.001$  and room temperature curable characteristics. Xylene and Dibutyltindilaurate have been used as solvent and curing agent respectively for the preparation of composites.

The desired weight percentage of filler CB is added into the solvent and sonicated for 10 minutes using ultrasonic bath for dispersing CB particles properly. This CB suspension is then added to the silicone-rubber paste and stirred for 10 minutes. The required amount of hardner (5% of SiR) is added to the mixture and stirred properly for 5 minutes. The resultant mixture is immediately poured into a rectangular mould ( $50 \text{ mm} \times 50 \text{ mm} \times 2 \text{ mm}$ ) and pressed for 8–10 hours for proper curing. After curing, the sheet is removed from the mould and kept for 24 hours in ambient conditions. The obtained sheet is cut into the desired dimensions for waveguide measurements for EM characterization in X (8.2–12.4 GHz) and Ku (12.4–18 GHz) bands of microwave frequency range. Samples with different loadings of CB from 1 wt% to 15 wt% in silicone-rubber are prepared with die press method. The samples prepared with 3 wt%, 5 wt%, 10 wt% and 15 wt% of nanosize carbon are named as  $S_1$ ,  $S_2$ ,  $S_3$  and  $S_4$ , respectively. Pure silicone rubber sample, named as  $S_0$ , is also prepared to compare the results.

### 2.2. Characterization of Composites

The structural characterization of the filler CB powder is carried out by powder X-ray diffraction performed on a Philip X'Pert Pro system while using  $\text{CuK}\alpha 1$  ( $\lambda = 1.54 \text{ \AA}$ ) radiation. Transmission Electron Microscope (TEM, JEOL 3010) and Scanning Electron Microscope (SEM, Carl Zeiss, EVO-MA 15) are used to analyze the size of filler particles and morphology of composite samples respectively. Four point resistivity probe and Electrometer (High Resistance meter) Model 6517A from Keithely are used for measurement of volume resistivity.

Electromagnetic parameters and shielding effectiveness measurements are carried out by waveguide transmission line technique using Vector Network Analyzer (Rohde & Schwarz, ZVM model) instrumentation over 8–18 GHz frequency range as shown in Figure 1. The system is calibrated using

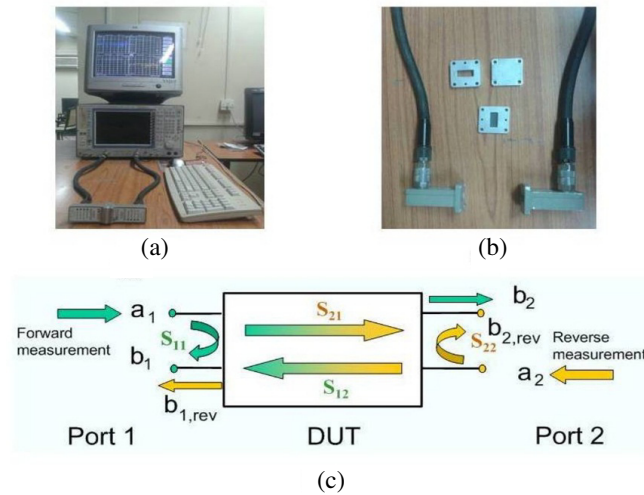


**Figure 1.** (a) Set up for measurement of EM parameters and SE. (b) Sample holder with calibration standards. (c)  $S$ -parameter flow graph.

Thru-Reflect-Line (TRL) calibration technique in X and Ku bands. The levels of isolation ( $S_{21}$ -parameter) are found  $\sim -80$  dB for perfect electric conductor (PEC). Rectangular samples of sizes  $22.86 \text{ mm} \times 10.16 \text{ mm}$  and  $15.80 \text{ mm} \times 7.9 \text{ mm}$  are cut from the prepared composites and measurements carried out in X and Ku bands to cover the frequency range 8–18 GHz.  $S$ -parameters (Reflection and Transmission) are measured in both bands. Complex permittivity and permeability properties are extracted from these parameters using Nicolson-Ross procedure [21]. Different components of SE viz. reflection, absorption and total SE are also calculated from the measured  $S$ -parameters.

### 3. RESULTS AND DISCUSSION

#### 3.1. Filler Material Characterization

Figure 2(a) shows the powder XRD spectrum of pure carbon black (CB) which is used as filler material in the present study. The pure hexagonal graphitic phase is seen from the spectrum. The average crystalline diameter determined from the XRD spectrum by using Debby Scherer equation is found in the range of 15–20 nm. The corresponding TEM image of powder is shown in Figure 2(b). From TEM image, it is observed that CB particles are distributed in the form of aggregates, wherein the individual particle size is found  $\sim 15$  nm. These aggregates due to high surface area result into enhanced interfacial polarization causing increased attenuation of the electromagnetic wave energy.

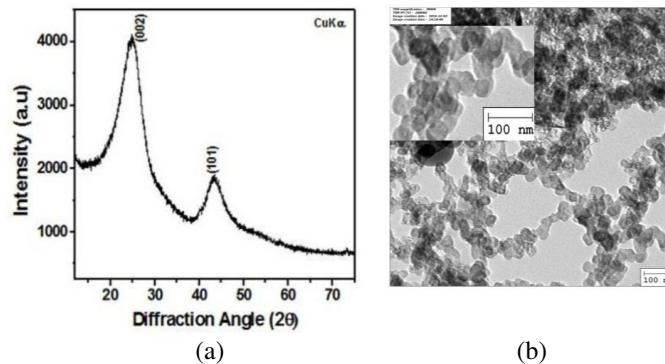


**Figure 2.** (a) Powder XRD spectrum and (b) TEM micrograph of pure CB.

### 3.2. Volume Resistivity and DC Conductivity of Composites

The volume resistivity of CB-SiR composites as a function of CB concentration is shown in Figure 3(a). Corresponding DC conductivity profile is shown in Figure 3(b).

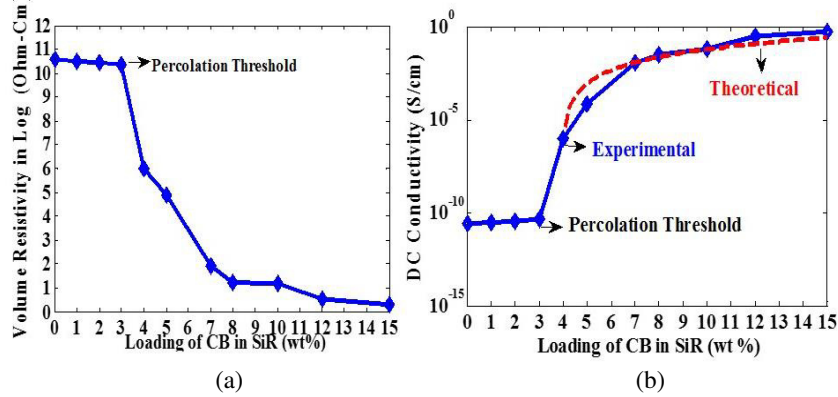


**Figure 3.** Effect of CB loading on (a) Volume resistivity (b) DC conductivity.

From Figure 3(a), it is observed that composites having 0–3 wt% CB loading show high resistivity of the order of  $10^{11} \Omega\text{cm}$ . However, increasing the concentration of CB up to 4 wt%, the resistivity value sharply decreases by nearly five orders of magnitude to around  $10^6 \Omega\text{cm}$ . With further increasing the CB content, the rate of decrease in resistivity with reference of CB concentration remains quite high up to loading of 8 wt%. Beyond 8 wt% CB concentration, rate of decrease in resistivity w.r.t. CB is very small, i.e., now the fall in resistivity is much less. The studies are continued up to 15 wt% of CB. The critical concentration level, where the system transforms from insulating to conducting stage, is known as percolation threshold. From the curve, percolation threshold is found at 3 wt%, and percolation zone can be defined in the range of 3–8 wt% loading of CB. Further, theoretical percolation threshold of CB as filler in polymer matrix can be explained by equation given by Janzen [22, 23]. The calculated value of percolation threshold is 3.6 wt% which closely matches with experimental value  $\sim 3.0$  wt% (Figure 3(a)) in the present study. Although the calculated value of percolation threshold is very close to the experimental data, selection of matrix and method of preparation of composites by proper dispersion of filler in matrix is very important to obtain low percolation threshold in the composites. We have achieved low percolation threshold by selecting appropriate CB with high surface area and high pore volume (DBP value) as filler material and room temperature curable silicone rubber (medium viscosity) as binder matrix.

Figure 3(b) shows the DC conductivity profile of the composites. The change in the conductivity beyond the percolation threshold is expressed using the following power law equation [24, 25].

$$\sigma = K(\rho - \rho_c)^t \quad (1)$$

where  $\sigma$  is the conductivity of composite,  $K$  the constant of proportionality,  $\rho$  the mass fraction of filler material,  $\rho_c$  the mass fraction of carbon black at the percolation threshold, and  $t$  the critical exponent which governs the scaling behaviour in the region  $\rho_c$ . The observed value of  $t = 2.96$  is found in the range of reported values 2 to 4.5 for such systems [26, 27].

### 3.3. Morphology Studies of Composites

In order to understand the low percolation threshold in composites, SEM micrographs are taken for the CB-SiR composites containing 0–15 wt% CB. Some of the representative images are shown at Figure 4. The SEM image of composite with 3 wt% loading shows change in morphology, wherein some aggregates are seen in contact with each other and a few others separated in the image (Figure 4(a)). With further increasing the loading of CB filler (5 wt% CB), closely spaced fine aggregates forming continuous network are observed in the image (Figure 4(b)). In 10 wt% composite (Figure 4(c)), these aggregates are found

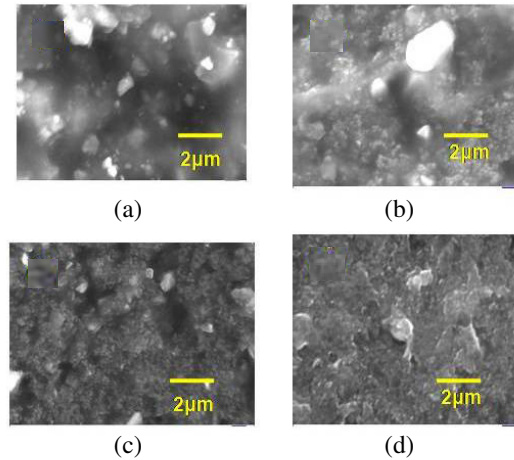


**Figure 4.** SEM Micrographs of CB-silicone rubber composites. (a) 3 wt%. (b) 5 wt%. (c) 10 wt%. (d) 15 wt%.

denser than the samples with lower concentrations. The composite with 15 wt% CB shows further change in morphology with layered structure (Figure 4(d)).

The insulating behaviour of composite with lower loading (1 wt% and 2 wt%) is observed due to insufficient network to conduct the electricity, as aggregates are largely spaced in the matrix. This behaviour continues up to 3 wt% loading of CB due to lack of continuous network. However, in 5 wt% composite, increase in dc electrical conductivity of the composites is observed due to formation of continuous network of aggregates which can provide effective conducting path [28]. Increase in the electrical conductivity of composites is observed at higher concentration of 10 wt% because of formation of strong chain structure of aggregates of CB. Further, for the composite with 15 wt% of CB, the flow of electron becomes much easier due to the formation of layer structure, which enhances the conductivity.

### 3.4. Complex Permittivity ( $\epsilon = \epsilon' - j\epsilon''$ ) and Permeability ( $\mu = \mu' - j\mu''$ ) Properties

The real ( $\epsilon'$ ) and imaginary ( $\epsilon''$ ) parts of complex permittivity of composite samples  $S_0$  to  $S_3$  are shown in Figures 5(a) and 5(b), respectively. From the figures, it is observed that both  $\epsilon'$  and  $\epsilon''$  values of composites increase with increasing the concentration of CB. The corresponding loss tangent ( $\tan \delta_e$ ) values also increase with CB content (Figure 5(c)). Values of  $\epsilon'$  and  $\epsilon''$  for pure silicone rubber (sample  $S_0$ ) are found  $\sim 3$  and  $\sim 0.01$ , respectively, over 8–18 GHz, whereas for sample  $S_1$  (3 wt% CB)  $\epsilon'$  and  $\epsilon''$  values are increased to  $\sim 5$  and  $\sim 1$ , respectively, and found almost constant over 8–18 GHz. With further increasing the concentration of CB (sample  $S_2$  – 5 wt%)  $\epsilon'$  and  $\epsilon''$  show dispersion characteristics with frequency and loss tangent values at  $\sim 0.45$ – $0.5$ . At further higher concentration of CB (sample  $S_3$  – 10 wt%), composite shows more dispersion characteristics with increased loss tangent values  $\sim 0.8$ – $0.9$  over 8–18 GHz. The dispersion behaviour of imaginary part of permittivity [29] in the composites is given as:

$$\epsilon'' = \frac{\sigma_{dc}}{\omega} + \epsilon''_{relax} \quad (2)$$

The enhanced values of loss factor in sample  $S_2$  and  $S_3$  are observed due to formation of conductive network between CB aggregates as depicted in SEM images resulting in increase in dc conductivity ( $\sigma_{dc}$ ). As a result, the dielectric loss of composites increases. EM characterization results of sample  $S_4$  (15 wt% CB) are found conducting in nature. Therefore, permittivity results are not shown in the figures given above. For composites below critical threshold, i.e., 3 wt%, the observed values of loss factor are related to the interfacial polarization which occurs due to combination of higher conducting filler (CB) with non-conducting binder matrix (SiR). Therefore, loss factor increases slightly ( $\epsilon''_{relax}$ ) for these composites. The magnetic permeability is found almost constant, i.e.,  $\mu \sim 1 - j*0$  for all samples, indicating dielectric nature of composites.

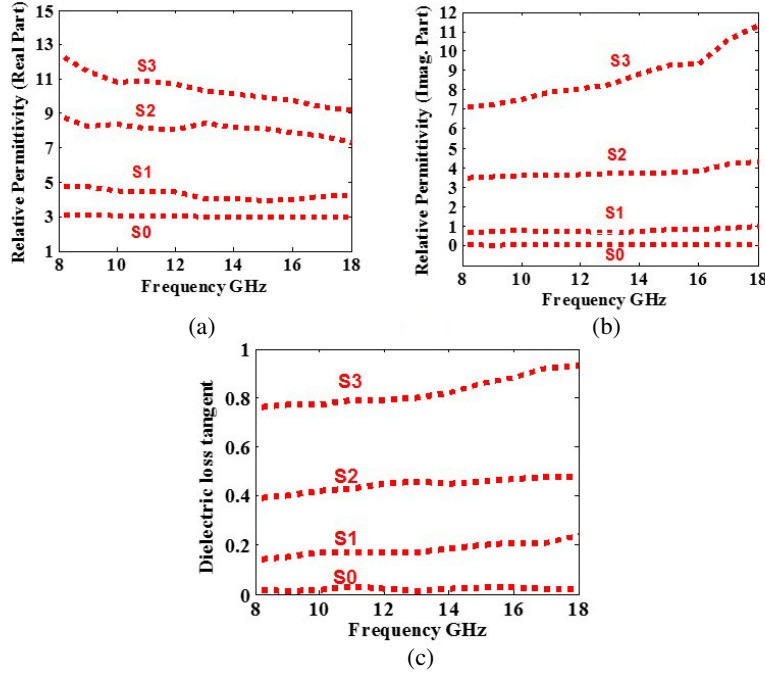


**Figure 5.** Complex permittivity vs. frequency. (a) Real part ( $\epsilon'$ ). (b) Imaginary part ( $\epsilon''$ ). (c) Dielectric loss tangent ( $\tan \delta_e$ ).

### 3.5. Microwave Absorption Properties

Reflection Loss (RL) of the composites as a microwave absorber is calculated using the measured data of complex relative permittivity ( $\epsilon$ ) and relative permeability ( $\mu$ ) based on transmission line model. The normalized input impedance ( $Z_n$ ), reflection coefficient ( $\Gamma$ ) and RL (in dB) for a PEC backed single layer absorber under normal incidence of EM wave are defined as [30]:

$$Z_n = \frac{Z_m}{Z_0} = \sqrt{\frac{\mu}{\epsilon}} \tanh \left[ j \left( \frac{2\pi f d}{c} \right) \sqrt{\mu \epsilon} \right] \quad (3)$$

$$\Gamma = \frac{Z_n - 1}{Z_n + 1} \quad (4)$$

$$R.L. = 20 \log_{10} |\Gamma| \quad (5)$$

where  $f$  is the frequency of the EM wave;  $d$  is the thickness of the absorber;  $c$  is the velocity of light in the free space;  $\epsilon$  and  $\mu$  are the relative complex permittivity & permeability;  $Z_0$  is the characteristic impedance of free space  $\sim 377 \Omega$ ;  $Z_m$  is the impedance of material;  $Z_n$  is the normalized input impedance.

Figure 6(a) shows the calculated RL (microwave absorption) values for samples  $S_0$ ,  $S_1$ ,  $S_2$  and  $S_3$  for composite thickness 2 mm.

For sample  $S_0$ , no absorption (RL  $\sim 0$  dB) and for sample  $S_1$  (3 wt% CB) very small absorption (RL  $< -5$  dB) are observed. For sample  $S_2$  (5 wt% CB) maximum RL  $\sim -29$  dB (absorption peak) is found at 13 GHz with  $> -10$  dB RL over 11–16 GHz frequency range (5 GHz bandwidth). However, in sample  $S_3$  (10 wt% CB), no such absorption peak is observed and RL response found almost flat in nature with values  $\sim -6$  to  $-10$  dB over 8–18 GHz. To understand the absorption behaviour of these composites, normalized impedance for a single layer absorber of 2 mm thickness is calculated using the permittivity and permeability data of all samples as shown in Figure 7(a). It is observed that for sample  $S_2$ , the value of  $Z_n$  is found  $\sim 0.93$  (close to 1) at 13 GHz frequency in comparison to other composite samples over 10–18 GHz, which provides better impedance match with free space impedance for EM waves to attenuate (Figure 7(b)). Similarly, for thickness 1.9 mm, the absorption peak with



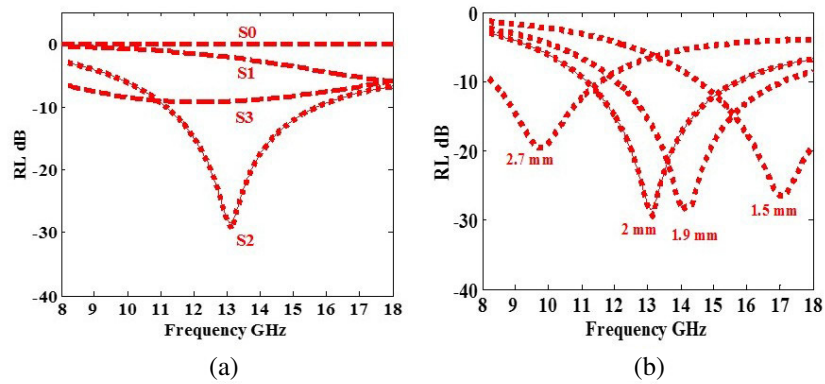


**Figure 6.** Reflection loss (RL) vs. frequency (a) RL of samples  $S_0$ – $S_3$  at thickness 2 mm (b) RL of sample  $S_2$  at different thicknesses.

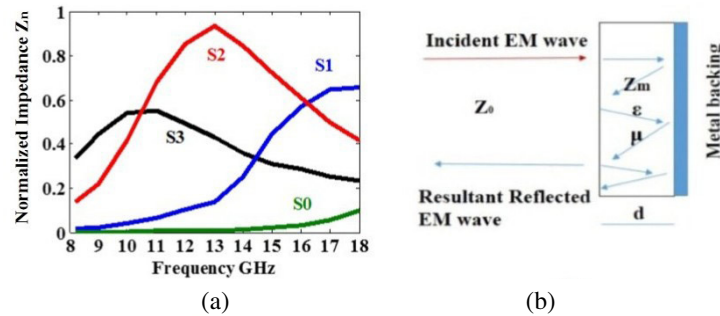


**Figure 7.** (a) Normalized impedance vs. frequency of all samples at thickness 2 mm. (b) Schematic of RL phenomenon of a single layer MW absorber.

maximum RL  $\sim -28$  dB is observed at 14 GHz, with more than 90% MW absorption (RL  $> -10$  dB) over 12–18 GHz (6 GHz BW).

Although sample  $S_3$  shows high value of loss tangent in comparison to sample  $S_2$  (Figure 5(c)), the EM wave reflects from the front surface of the absorber (Figure 7(b)), due to major contribution from impedance mismatch (Figure 7(a)). As a result, the absorption of microwave energy decreases in sample  $S_3$ . Therefore, sample  $S_2$  is selected for calculation of RL values at different thicknesses of the absorber. The calculated RL values for this sample are shown in Figure 6(b). The absorber of this composition is found to give tunable RL values over 8–18 GHz by varying thickness from 1.5 to 2.7 mm. The absorption bandwidth ( $> 90\%$  MW absorption) of absorber is found  $\sim 6$  GHz and  $\sim 4$  GHz for absorber thickness of 1.9 mm and 2.7 mm in Ku and X bands, respectively. In earlier report [12], narrow bandwidth of absorption ( $\sim 1.2$  GHz) was reported by taking CB as filler in composites. Further, the increase in the bandwidth of absorption was observed by taking additional filler SiC (50 wt%) along with CB (5 wt%). Similar observations are reported in [3], wherein other filler materials viz. BaTiO<sub>3</sub>, Fe(Co)<sub>5</sub>, nanosize Fe and ferrites were used along with CB in composites to achieve enhanced bandwidth. The other filler materials, with higher density, result in the increase in the overall weight of the composites to achieve the same performance. Therefore, there is always compromise between absorption performance and weight penalty of absorber. The high absorption bandwidth and low weight penalty are always preferred for practical applications. In our studies, we can achieve light weight absorber having large bandwidths  $\sim 6$  GHz in Ku-band and  $\sim 4$  GHz in X-band with more than 90% microwave absorption (RL  $> -10$  dB) using very low concentration of CB (5 wt%) in the composites without any additional fillers.

### 3.6. Shielding Effectiveness (SE)

The shielding effectiveness of a material is measured in terms of reduction in magnitude of incident power/field upon transition across the shield material. The total shielding effectiveness ( $SE_T$ ) is expressed as [31]:

$$SE_T = SE_R + SE_A + SE_M = 10 \log_{10}[P_T/P_I] = 20 \log_{10}[E_T/E_I] = 20 \log_{10}[H_T/H_I] \quad (6)$$

Three different mechanisms, namely reflection ( $R$ ), absorption ( $A$ ) and multiple internal reflections ( $M$ ), contribute towards overall attenuation. Experimentally, shielding effectiveness is measured using Vector Network Analyzer (VNA) system.  $S$ -parameters ( $S_{11}$  &  $S_{21}$ ) are measured with VNA system. Further, reflection ( $SE_R$ ), absorption ( $SE_A$ ) components of SE and total shielding effectiveness ( $SE_T$ ) are calculated using these parameters as [32, 33]:

$$SE_R = 10 \log 10(1 - R) = 10 \log 10 (|1 - S_{11}|^2) \quad (7)$$

$$SE_A = 10 \log 10(1 - A_e) = 10 \log 10 \left[ \frac{T}{1 - R} \right] \quad (8)$$

$$SE_T = 10 \log 10|T| = 10 \log 10|S_{21}|^2 = SE_R + SE_A \quad (9)$$

Results of shielding effectiveness for samples  $S_0$ – $S_4$  measured in X and Ku bands are shown in Figure 8. Figures 8(a) and 8(b) show the reflection component ( $SE_R$ ), and Figures 8(c) and 8(d) show the absorption component of SE ( $SE_A$ ) over X and Ku bands. From the figures it is observed that  $SE_R$  decreases with increasing the frequency. Figures 8(e) and 8(f) show the variation of total shielding effectiveness ( $SE_T$ ) with frequency in X and Ku bands. The total shielding effectiveness is determined from the measured values of transmission parameters ( $S_{21}$ ) as per Eq. (9). From the figures, it is clear that SE of the composites increases with increasing the loading of CB in matrix. The composite with 15 wt% of CB (samples  $S_4$ ) shows  $\sim -40$  dB SE over X and Ku bands. The observed Shielding effectiveness of composites results from high values of electrical conductivity of samples, which

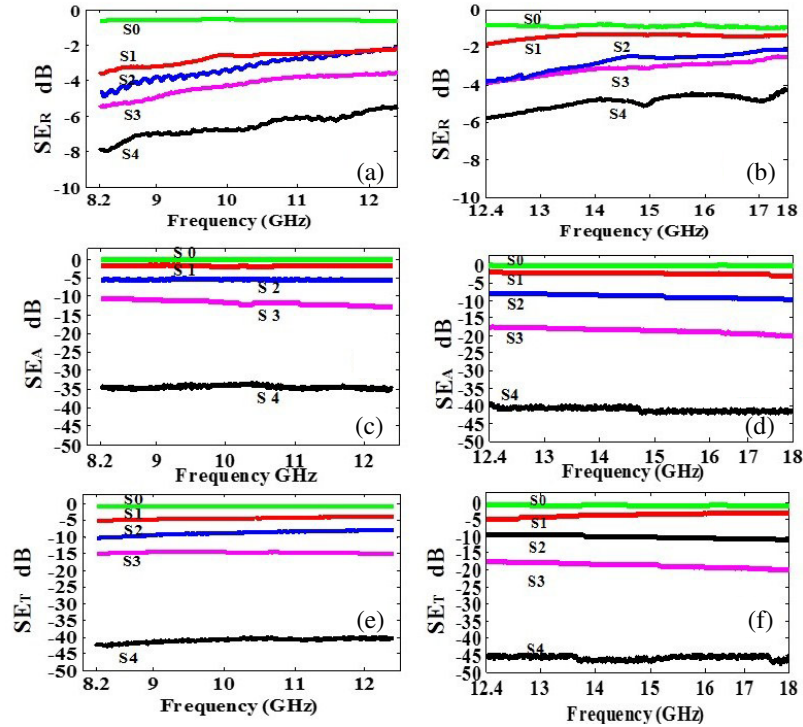


**Figure 8.** Shielding effectiveness vs. frequency. (a)  $SE_R$  in X-band. (b)  $SE_R$  in Ku-band. (c)  $SE_A$  in X-band. (d)  $SE_A$  in Ku-band. (e)  $SE_T$  in X-band. (f)  $SE_T$  in Ku-band.



is attributed to layer morphology in this composition as seen in SEM image. In the previous studies, using nanosize CB with CNTs and short carbon fibers, a maximum SE of  $\sim -30$  dB was achieved [15–17], but at higher content of CB.

3.6.1. Effect of Composite Thickness on SE

Figure 9(a) and 9(b) show the effect of composite thickness on shielding effectiveness and reflectivity for 15 wt% CB composite in 8–18 GHz. The shielding effectiveness increases from  $-15$  dB to  $-40$  dB by varying the thickness from 1 mm to 2.8 mm respectively for this composition. Further increasing the thickness ( $\sim 3.3$  mm), the transmission values approach PEC response (Figure 9(a)). Reflectivity profile of the composite does not show any significant change (values are found within  $\sim 1$ – $2$  dB) with thickness (Figure 9(b)). From the above studies, it is clear that dominant phenomenon for increase in shielding effectiveness is absorption of microwave energy within the composites.

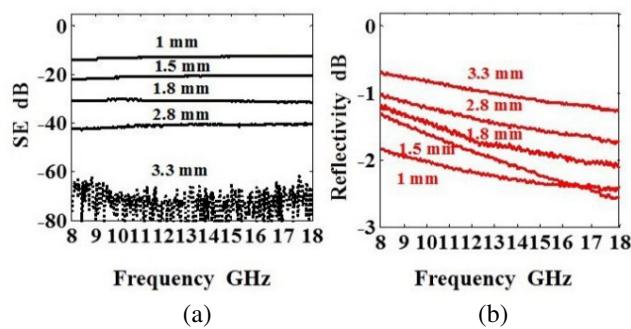


Figure 9. Effect of composite thickness on (a) shielding effectiveness, (b) reflectivity.

3.6.2. Effect of Filler Content on SE

The SE of composite depends on the conductivity, thickness of sample and frequency of operation. To find SE values of the composites for different contents of CB, we plot graphs for different thicknesses of the composites as shown in Figure 10. It is observed that SE values increase with increasing CB content in the composites irrespective of thickness. However, the values are found more for higher thickness. From these curves, loading of CB required to get desired SE values can be determined for a given thickness and frequency.

Details of conductivity, RL and SE values of composites having thickness 2.8 mm are summarized at Table 1.

Table 1. Conductivity, RL and SE of Composites (thickness 2.8 mm).

Sample	Composition	Conductivity (S/cm)	Tangent Loss ( $\tan \delta_e$ )	RL (-dB) at 13 GHz	SE (-dB)
$S_0$	0 wt%	$2.63 \times 10^{-11}$	$\sim 0$	$\sim 0$	$\sim 0$
$S_1$	3 wt%	$6.50 \times 10^{-11}$	$\sim 0.2$	$\sim 2$	$\sim 5$
$S_2$	5 wt%	$1.25 \times 10^{-6}$	$\sim 0.4$	$\sim 29$	$\sim 10$
$S_3$	10 wt%	$5.95 \times 10^{-2}$	$\sim 0.8$	$\sim 9$	$\sim 15$
$S_4$	15 wt%	$5.70 \times 10^{-1}$	-	-	$\sim 40$

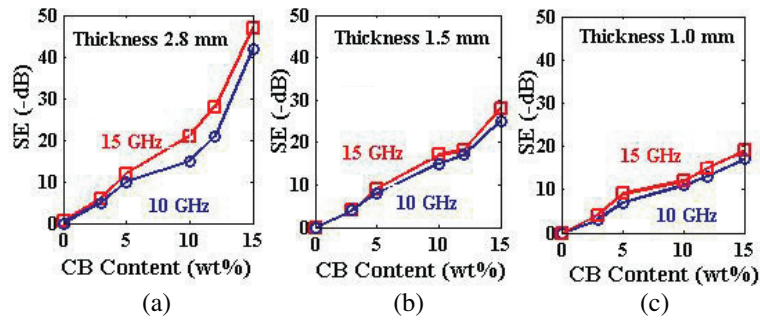


**Figure 10.** SE vs. content of CB (wt%) at thickness (a) 2.8 mm, (b) 1.5 mm, (c) 1.0 mm.

#### 4. CONCLUSION

Conducting carbon black (CB) — silicone rubber composites are prepared, and their morphology, DC conductivity, dielectric & microwave absorption properties and shielding effectiveness are investigated in the frequency range of 8–18 GHz. The volume resistivity and DC conductivity measurements suggest low percolation threshold at 3 wt% of CB for these composites and percolation zone found to be 3–8 wt% loading of CB. The composites with 5 wt% loading of CB show more than 90% absorption ( $RL > -10$  dB) in X and Ku bands with thicknesses 2.7 mm and 1.9 mm, respectively. Further, Shielding Effectiveness (SE) studies of composites are carried out with different concentrations of CB. An SE of  $\sim -40$  dB is achieved at 15 wt% CB-rubber composites with thickness 2.8 mm over the frequency range 8–18 GHz. The SE increases with increasing the thickness of the composites. SE values can be tuned in the range of  $-15$  dB to  $-40$  dB by varying the thickness from 1 mm to 2.8 mm for the same composition. The prepared composites with selected filler concentration have potentials for microwave absorption in Stealth Technology and also for EMI shielding of various equipments in military and civil areas.

#### ACKNOWLEDGMENT

The authors are thankful to Mr. Manish Kumar, Radiation & Solar Devices Group for support in DC conductivity measurements and Mrs. Anjali Bhatia, Head, Camouflage Division and Mr. V. S. Chauhan, Microwave Group, Defence Laboratory, Jodhpur for their valuable suggestions and technical support during experimental work.

#### REFERENCES

1. Knott, E. F., J. F. Shaeffer, and M. T. Tully, *Radar Cross Section*, Artech House Inc., Norwood, 1993.
2. Vinoy, K. J. and R. M. Jha, *Radar Absorbing Materials: From Theory to Design and Characterization*, Kluwer Academic Publishers, Boston, MA, 1996.
3. Qin, F. and C. Brosseau, "A review and analysis of microwave absorption in polymer composites filled with carbonaceous particles," *Journal of Applied Physics*, Vol. 111, 061301-24, 2012.
4. Singh, V. K., A. Shukla, M. K. Patra, L. Saini, R. K. Jani, S. R. Vadera, and N. Kumar, "Microwave absorbing properties of thermally reduced graphene oxide/nitrile butadiene rubber composite," *Carbon*, Vol. 50, 2202–2208, 2012.
5. Bhattacharya, P., S. Sahoo, and C. K. Das, "Microwave absorption behavior of MWCNT based nanocomposites in X-band region," *Express Polymer Letters*, Vol. 7212-223, 2013.
6. Zhang, W., Y. Xu, L. Yuan, J. Cai, and D. Zhang, "Microwave absorption and shielding property of composites with FeSiAl and carbonaceous materials as filler," *Journal of Material Science and Technology*, Vol. 28, 913–919, 2012.

7. Xu, Y., D. Zhang, J. Cai, L. Yuan, and W. Zhang, "Effect of multi-walled carbon nanotubes on the electromagnetic absorbing characteristics of composites filled with Carbonyl Iron Particles," *Journal of Material Science and Technology*, Vol. 28, 34–40, 2012.
8. Joseph, N., C. Janardhanan, and M. T. Sebastian, "Electromagnetic interference shielding properties of butyl rubber-single walled carbon nanotube composites," *Composite Science and Technology*, Vol. 101, 139–144, 2014.
9. Savi, P., M. Miscuglio, M. Giorcelli, and A. Tagliaferro, "Analysis of microwave absorbing properties of epoxy MWCNT composites," *Progress In Electromagnetic Research Letters*, Vol. 44, 63–69, 2014.
10. Saib, A., L. Bednarz, R. Daussin, C. Bailly, X. Lou, J. M. Thomassin, C. Pagnoulle, C. Detrembleur, R. Jerome, and I. Huynen, "Carbon nanotube composites for broadband microwave absorbing materials," *IEEE Transactions on Microwave Theory and Techniques*, Vol. 54, 2745–2754, 2006.
11. Al-Hartomy, O. A., A. Al-Ghamdi, N. Dishovsky, R. Shtarkova, V. Iliev, I. Mutlay, and F. El-Tantawy, "Dielectric and microwave properties of natural rubber based nanocomposites containing grapheme," *Materials Sciences and Applications*, Vol. 3, 453–459, 2012.
12. Liu, X., Z. Zhang, and Y. Wu, "Absorption properties of carbon black/silicon carbide microwave absorbers," *Composites: Part B*, Vol. 42, 326–329, 2011.
13. Wang, M., Y. Duan, S. Liu, X. Li, and Z. Ji, "Absorption properties of carbonyl-iron/carbon black double-layer microwave absorber," *Journal of Magnetism and Magnetic Materials*, Vol. 321, 3442–3446, 2009.
14. Vinayasree, S., M. A. Soloman, V. Sunny, P. Mohanan, P. Kurian, P. A. Joy, and M. R. Anantharaman, "Flexible microwave absorbers based on barium hexaferrite, carbon black, and nitrile rubber for 2–12 GHz applications," *Journal of Applied Physics*, Vol. 116, 24902–24907, 2014.
15. Wang, X., "Investigation of electromagnetic shielding effectiveness of nano-structural carbon black-ABS composites," *Journal of Electromagnetic Analysis and Applications*, Vol. 3, 160–164, 2011.
16. Dinesh, P. G., N. M. Renukappa, T. Pasang, M. Dinesh, and C. Rangananthaiah, "Effect of nanofillers on conductivity and electromagnetic interference shielding effectiveness of high density polyethylene and polypropylene nanocomposites," *European Journal of Advances in Engineering and Technology*, Vol. 1, 16–28, 2014.
17. Das, N. C., D. Khastgir, T. C. Chaki, and A. Chakraborty, "Electromagnetic interference shielding effectiveness of carbon black and carbon fiber filled EVA and NR based composites," *Composites Part A: Applied Science and Manufacturing*, Vol. 31, 1069–1081, 2001.
18. Li, L. and D. D. L. Chung, "Electrical and mechanical properties of electrically conductive polyethersulfone composite," *Composites*, Vol. 25, 215–224, 1994.
19. Chung, D. D. L., "Electromagnetic interference shielding effectiveness of carbon materials," *Carbon*, Vol. 39, 279–285, 2001.
20. Shui, X. and D. D. L. Chung, "Nickel filament polymer-matrix composites with low surface impedance and high electromagnetic interference shielding effectiveness," *Journal of Electronic Materials*, Vol. 26, 928–934, 1997.
21. Nicolson, A. M. and G. F. Ross, "Measurement of the intrinsic properties of materials by time domain techniques," *IEEE Trans. on Instrumentation and Measurements*, Vol. 19, 377, 1970.
22. Janzen, J., "On the critical conductive filler loading in antistatic composites," *Journal of Applied Physics*, Vol. 46, 966–969, 1975.
23. Donnet, J. B., R. C. Bansal, and M. J. Wang, *Carbon Black*, 2nd Edition, Marcel Dekker Inc., New York, 1993.
24. Stauffer, D. and A. Aharony, *Introduction to Percolation Theory*, 2nd Edition, Taylor & Francis, London, 1994.
25. Li, H., X. Qian, T. Li, and Y. Ni, "Percolation for coated conductive paper: electrical conductivity as a function of volume fraction of graphite and carbon black," *BioResources*, Vol. 10, 4877–4885, 2015.

26. Foulger, S. H., "Reduced percolation threshold of immiscible conductive blends," *Journal of Polymer Science Part: B Polymer Physics*, Vol. 37, 1899–1910, 1999.
27. Belberg, I., "Tunneling and non-universal conductivity in composite materials," *Physical Review Letters*, Vol. 59, 1305, 1987.
28. Wessling, B., "Electrical conductivity in heterogeneous polymer systems V(1): Further experimental evidence for a phase transition at the critical volume concentration," *Polymer Engineering Science*, Vol. 31, 1200-6, 1991.
29. Achour, M. E., M. Malhi, J. L. Miane, F. Carmona, and F. Lahjomri, "Microwave properties of carbon black-epoxy resin composites and their simulation by means of mixture laws," *Journal of Applied Polymer Science*, Vol. 73, 969, 1999.
30. Kim, S. S., S. B. Jo, H. I. Gueon, K. K. Choi, J. M. Kim, and K. S. Churn, "Complex permeability and permittivity and microwave absorption of ferrite-rubber composite in X-band frequencies," *IEEE Trans. on Magnetism*, Vol. 27, 5462, 1991.
31. Paul, C. R., *Introduction to Electromagnetic Compatibility*, 2nd Edition, John Wiley and Sons, New York, 2005.
32. Saini, P., V. Choudhary, B. P. Singh, R. B. Mathur, and S. K. Dhawan, "Enhanced microwave absorption behavior of polyaniline-CNT/polystyrene blend in 12.4–18 GHz range," *Synthetic Metals*, Vol. 161, 1522–1526, 2011.
33. Pande, S., B. P. Singh, R. B. Mathur, T. L. Dhami, P. Saini, and S. K. Dhawan, "Improved electromagnetic interference shielding properties of MWCNT-PMMA composite using layered structure," *Nanoscale Research Letters*, Vol. 4, 327–334, 2009.